ACS APPLIED MATERIALS & INTERFACES

Research Article

www.acsami.org

Method for Measuring the Distribution of Adhesion Forces on Continuous Nanoscale Protrusions Using Carbon Nanofiber Tip on a Scanning Probe Microscope Cantilever

Norihiro Shimoi* and Daisuke Abe

Graduate School of Environmental Studies, Tohoku University 6-6-20 Aoba, Aramaki, Aoba-ku, Sendai 980-8579, Japan

ABSTRACT: The adhesion force on surfaces has received attention in numerous scientific and technological fields, including catalysis, thin-film growth, and tribology. Many applications require knowledge of the strength of these forces as a function of position in three dimensions, but until now such information has only been theoretically proposed. Here, we demonstrate an approach based on scanning probe microscopy that can obtain such data and be used to image the three-dimensional surface force field of continuous nanoscale protrusions. We present adhesion force maps with nanometer and nanonewton resolution that allow detailed characterization of the interaction between a surface and a thin carbon nanofiber (CNF) rod synthesized by plasma-enhanced chemical vapor deposition (PECVD) at the end of a tip on a scanning probe microscope cantilever in three dimensions. In these maps, the positions of all continuous nanoscale protrusions are identified and the differences in the adhesive forces among limited areas at inequivalent sites are quantified.

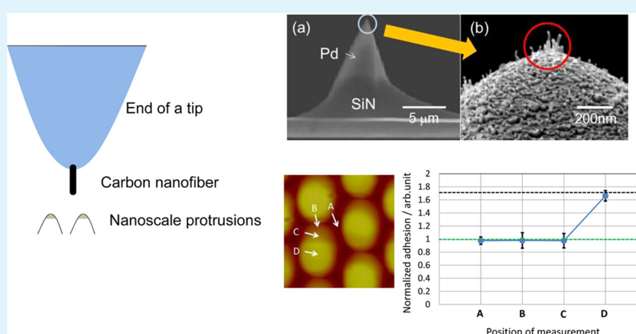

KEYWORDS: *carbon nanofiber, Pd nanoparticle, scanning probe microscope, adhesion force, nanonewton*

1. INTRODUCTION

The adhesion force refers to the attractive interaction between dissimilar surfaces. Adhesion plays a critical role in many areas of technology, ranging from the design of a parting agent in a transfer film with nanostructures to the use of actuators in microelectro-mechanical systems (MEMS).[1] In all cases, the adhesion must be controlled.[2] For instance, in the case of a transfer film with nanostructures, a lack of adhesion control results in low-quality transference.[3] The throughput in such a system is severely affected by weak adhesion between a mold and a transfer film. This weak adhesion can easily lead to the removal of a film with good patterned surface reliability.

Transfer films, such as the one used in this study, which has continuous nanoscale protrusions and is used as an antireflection (AR) layered film,[4−8] have only been recently developed. The nanostructured surface formed by the transcription of a light-curing acrylic resin and structured by a mold with nanoscale hollows, an SEM image of which is shown in Figure 1, exhibits a gradual change in the refractive index across the interface, leading to low reflectance over broad ranges of wavelengths and angles of incidence. Continuous nanoscale protrusions are a well-known technology used in wideband optical devices owing to their capability of reducing glare and enhancing the transmittance of light, but there have been few reports on their manufacturability or the efficiency of their properties. In addition, the pitch of these nanostructures must be sufficiently smaller than the wavelength of visible light. Such optical devices are fabricated using electron beam lithography[9] or laser beam interference[10] methods. However, these two methods are expensive and time-consuming; thus, the fabrication scale is still limited to less than one inch. These samples were imprinted and shaped by a mold with a nanoscale pattern of hollows. Each protrusion has a 100 nm diameter at its bottom and a height of 100 nm. The protrusions are aligned uniformly and hexagonally with a distance of approximately 200 nm between adjacent protrusions. The reflectance of the bell-shaped protrusions, such a structure is called a motheye structure, is constant in the visible range and the average reflectance is approximately 0.1%.

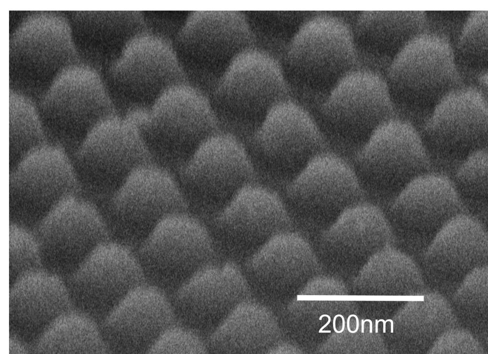

Figure 1. SEM image of nanoscale protrusions.

Received: February 11, 2015
Accepted: June 4, 2015
Published: June 4, 2015

© 2015 American Chemical Society

DOI: 10.1021/acsami.5b01307
ACS Appl. Mater. Interfaces 2015, 7, 13776−13781

The surface adhesion of continuous nanoscale protrusions can be tuned by structuring surfaces on the nanoscale. The effect of the nanoscale height on the adhesion force has been analyzed in several theoretical studies. The principal parameters used in most of these studies are the root-mean-square (RMS) roughness, that is, the standard deviation of the height, and the average roughness (R_a) of the surface. Both these parameters were used by Macdonald et al. to study the roughness of a carbon nanotube surface.[11] In an analysis by Persson and Tosatti,[12] the length scale of the height variation was also considered. A fluorinated compound is usually used as a parting agent to make it easy to remove a film from a mold without damage. When the agent in the film is uniformly distributed in the resin, the nanoscale structure can be imprinted uniformly from a mold. Research on nanoscale structures using a scanning probe microscope (SPM) has also been reported.[13] This measurement method can be used to analyze the surface morphology and shape of a continuous nanoscale surface. However, since not only the morphology but also the energy of the surface affects the adhesion, electrostatic contributions and van der Waals forces must be taken into account in such research. Under ambient conditions, if a fluorinated compound is homogeneously dispersed into the resin, a layer of water or oil from the fingers remains on the nanostructure surfaces owing to the capillary phenomenon. The pressure drop across the meniscus gives rise to the capillary effect, which significantly contributes to the adhesion. Several experimental and theoretical studies[14−25] have been devoted to studying the capillary effect under controlled humidity. They have demonstrated the sensitivity of the capillary force to both the relative humidity and the shape of the SPM tip. The majority of adhesion studies have been performed with a spherical SPM tip, that is, by attaching a small spherical particle on a planar substrate. In this study, to analyze adhesion force maps with nanometer and nanonewton resolution, we prepared a hydrophilic film by precipitation to enable the inhomogeneous dispersion of a parting agent on top of the film, allowing the film to absorb a layer of water or oil. This inhomogeneous transfer film should result in a curved meniscus between the film and SPM tip.

Some researchers have measured the relationship between the adhesion force and the position on a nanoscale protrusion using an SPM tip.[26,27] Small flat SPM tips have only been used in a few experiments[28,29] to study adhesion behavior. Ando[28] measured the effect of condensed water on the friction and adhesion forces on an array of hemispherical nanoscale asperities on a transparent film produced by a continuous coating process with transcription.

In this study, we attempted to use an SPM tip comprising a thin rod of less than 50 nm diameter to analyze the surface energy on a surface with an uneven morphology and continuous nanoscale protrusions.

For such a geometry, the surface energy between a smooth substrate and an SPM tip significantly differs from that between the surface of a protrusion and a spherical tip. In the latter case, the position of the neck is directly determined by the geometry, while for two surfaces, the location of neck formation is determined by a stochastic process. Despite this uncertainty in neck formation, the existence of many relevant technological applications means that it is much more appropriate to consider the interaction of an SPM tip with a substrate.

In this study, it was necessary to uniformly control the distribution of hydrophilic and hydrophobic layers in the nanoscale protrusions to measure the structure morphology and surface energy of the protrusions. Figure 2 shows ideal protrusions consisting of a hydrophilic layer on a hydrophobic layer.

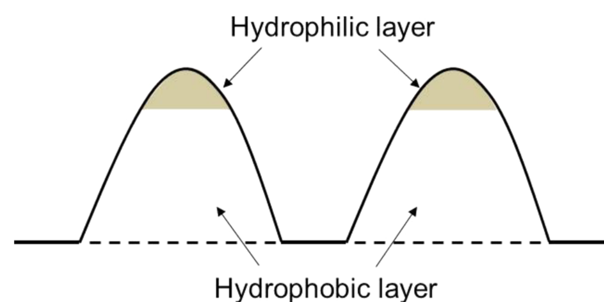

Figure 2. Schematic structure of ideal nanoscale protrusions.

2. EXPERIMENTAL SECTION

2.1. Preparation of Carbon Nanofiber Tip on an SPM Cantilever.

The method used to investigate the distribution of hydrophilic and hydrophobic layers involves measurement of the adhesion force using a contact−mode atomic force microscope (AFM) (Nanoscope IIIa, Bruker). The tip on an SPM cantilever, however, is too large compared with nanoscale protrusions; the schematic drawings in Figure 3a−d shows the physical relationship between the tip and nanoscale protrusions. The tip on an SPM cantilever has a quasi-pyramidal or conical shape, as shown in Figure 3b−d, and cannot reach the bottom of the valley between neighboring protrusions because the tip is larger than the concave spaces between the nanoscale protrusions. Thus, the adhesion force curve cannot be measured normally on the surface of protrusions. It is therefore necessary to bifurcate the protrusions to access the surface from the bottom to the top of the protrusions. To overcome this problem, the authors employ a thin carbon nanofiber (CNF) rod synthesized by chemical vapor deposition (CVD) at the end of a tip, which can easily reach the bottom of an array as shown in Figure 4. The attachment of carbon nanorods to SPM tips using different techniques has been reported by several groups.[30,31] We attempted to measure the shapes of continuous nanoscale protrusions with a thin CNF rod grown by CVD attached to the end of an SPM tip.

The roughness of the samples was determined by analyzing many topographic AFM images. The AFM images in this study were recorded in the contact mode using a silicon nitride (Si_3N_4) probe (D-NP-S, Bruker) with a CNF rod attached at the end of the tip. The silicon nitride probe employed as a cantilever in AFM serves as a spring in the stylus method. Generally, the stylus method can not only obtain a surface profile in a single scan but also acquire three-dimensional information on the surface of a sample by scanning the sample in the XYZ direction. It is important to measure the surface profiles of nanoscale protrusions with narrow hollows between protrusions and examine the force curve.

We attempted to fabricate a thin CNF rod at the end of a tip using a plasma-enhanced chemical vapor deposition (PECVD) system. Figure 5 shows a schematic diagram of the PECVD and sputtering system[32,33] used in this study. A tip covered with palladium (Pd) on a silicon nitride tip was used as the substrate for the growth of thin CNF rods as shown in Figure 6a. The Pd substrate acted as a catalyst for CNF growth by PECVD at 773 K using acetylene and ammonia at 72 Pa with a flow ratio of 1:2 as deposition gases. In this case, CNFs of approximately 30 nm diameter and 100−150 nm length were grown as shown in Figures 6b and 7.

Figure 7 shows a cross-sectional transmission electron microscope (TEM) image and a schematic image of synthesized CNFs of approximately 200 nm length. CNFs having a cup-stacking structure capped with Pd nanoparticles were synthesized on a Pd substrate at the end of the tip by PECVD under the above-mentioned conditions.

DOI: 10.1021/acsami.5b01307
ACS Appl. Mater. Interfaces 2015, 7, 13776−13781

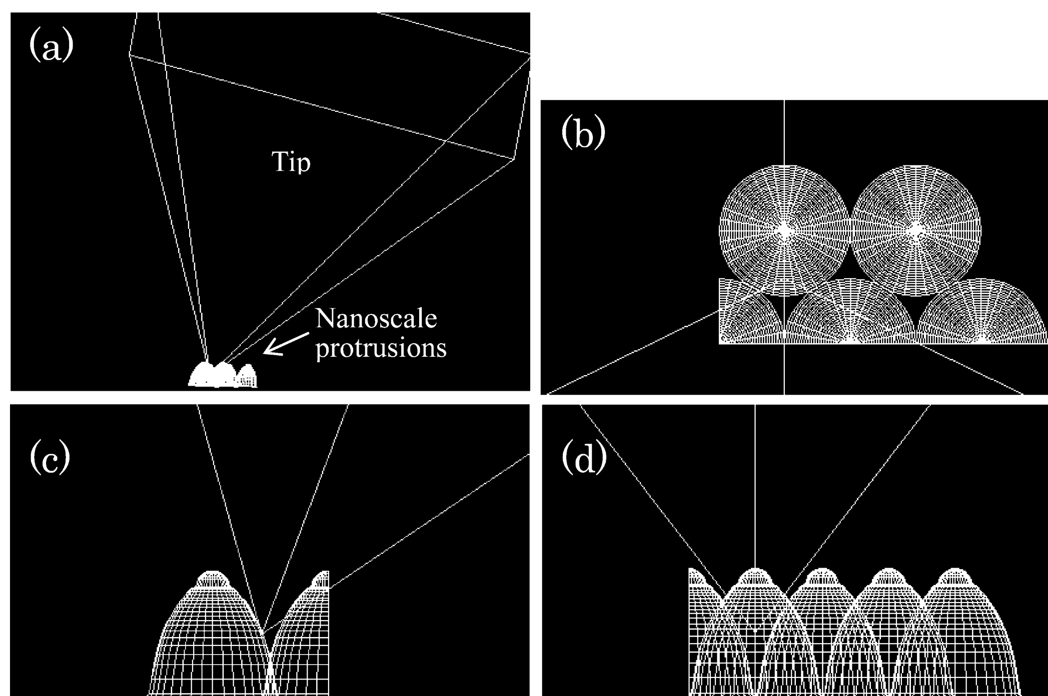

Figure 3. Scale comparison between nanoscale protrusions and the tip of a probe: (a) bird's-eye view of nanoscale protrusions and cantilever, (b) top view, (c) side view (enlargement of panel a), and (d) view from the other side.

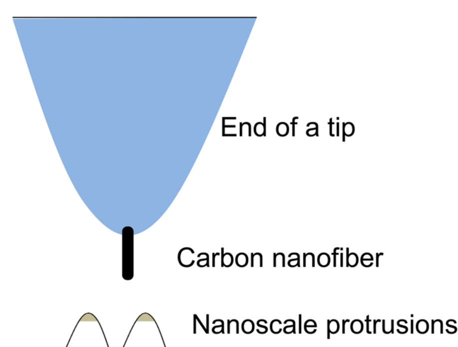

Figure 4. Schematic showing measurement employing CNF at the end of a tip.

It was found that the CNFs with nanoscale Pd particles at their ends were oriented vertically on the Pd substrate as schematically shown in Figure 6b.

2.2. Measurement for Imaging and Force-Curve Spectroscopy. In this study, the AFM scanning area was fixed at $3 \times 3\ \mu m^2$ and the imaging parameters were set to a scan rate of 1.00 Hz, an amplitude set point of 1.8−2.1 V, and a gain value of 3−5. The tuning of the cantilever was controlled to approximately 250 kHz. The principle of force curve spectroscopy can be schematically demonstrated by a force−distance curve, which shows the observed cantilever deflection (i.e., force) versus the displacement of the cantilever (e.g., ref 26). Force−distance curves using the distance between the point of maximum deflection of the cantilever before retraction and the zero-deflection point were obtained with a contact−mode AFM (Nanoscope IIIa) using a CNF tip prepared as described in section 2.1 on a cantilever. The force subjected to by the tip was evaluated by multiplying the recorded deflection by the spring constant of the cantilever. The spring constant of a cantilever is of fundamental importance to users of AFMs, and the accuracy of the spring constant of the cantilevers has been previously reported.[34−39] In this study, the spring constant (normal component) of the cantilever was 0.56 N/m, the value quoted by the manufacturer (Bruker). A sweep time of 5 s was used to record the force−distance curve.

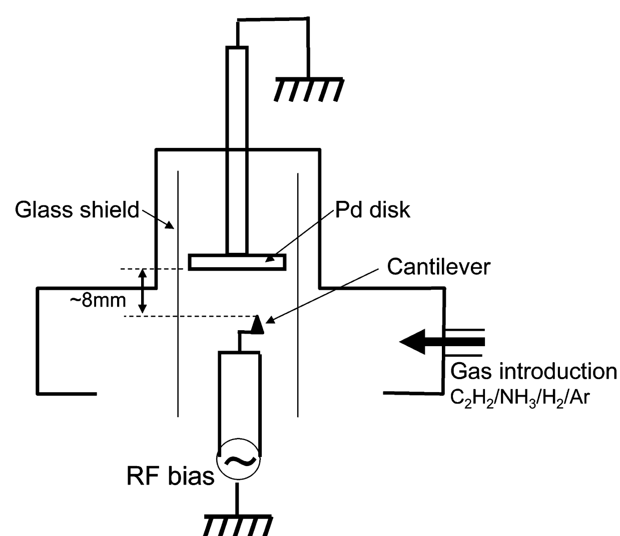

Figure 5. Schematic diagram of PECVD and sputtering system used in this study. High-density DC plasma was excited near a specimen at a low gas pressure (72 Pa). Acetylene (C_2H_2) and ammonia (NH_3) gases were introduced from the gas introduction pipe.

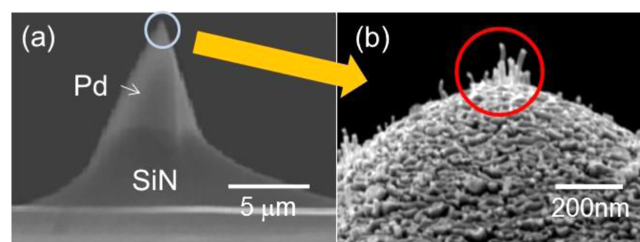

Figure 6. SEM images of a tip and CNFs: (a) tip covered with palladium by evaporation and (b) CNFs at the end of the tip.

DOI: 10.1021/acsami.5b01307
ACS Appl. Mater. Interfaces 2015, 7, 13776−13781

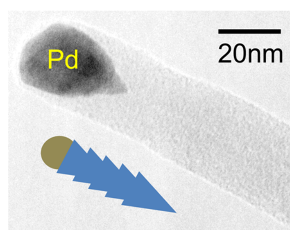

Figure 7. TEM image and schematic image of a CNF on a Pd substrate.

The adhesion measurements using a contact mode AFM were performed under controlled humidity. This was realized by placing the AFM in an environmental chamber with a controlled and adjustable air flow. Dry nitrogen was flowed into the chamber while measuring the morphology and surface energy on the nanoscale protrusions.

3. RESULTS AND DISCUSSION

Figure 8 shows the relationship between the angle between the tip and the direction perpendicular to a sample surface and the

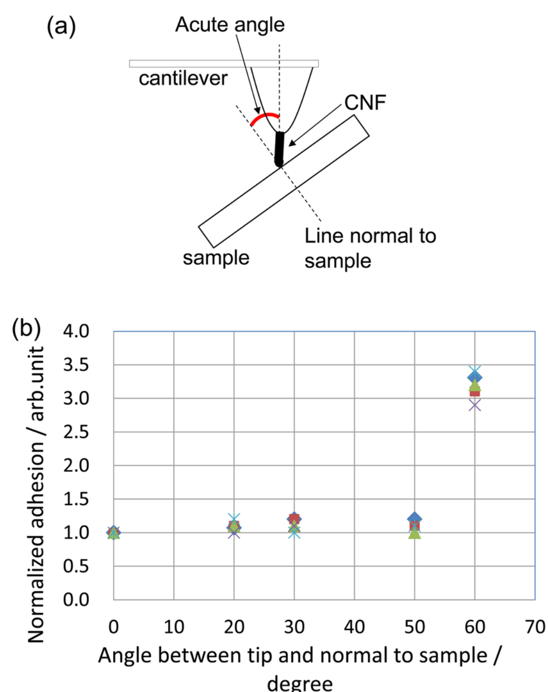

Figure 8. Relationships of contact angle between a CNF tip and measurement sample. (a) Schematic diagram of measurement setup with a probe employing CNF. (b) Relationship between normalized adhesion force and contact angle between cantilever and sample.

adhesion force normalized by its value perpendicular to the sample. When the top of the CNF tip on a cantilever comes in contact with a continuous nanoscale protrusion on a sample, the CNF tip is not normal to the sample surface. The angle between the CNF tip and the direction perpendicular to a film sample is indicated as the acute angle in Figure 8a. Figure 8b shows the dependence of the normalized adhesion force on the inclination angle for some different films. A polyethylene terephthalate (PET) film, a polycarbonate (PC) film, a fluorine compound film, a film with sputtered indium tin oxide, and a film with sputtered silicon oxide were chosen for measurement; some of the films included a layer of fluorinated ether chains as the parting agent on the substrate. When the angle is 0°, the adhesion force of the films is normalized to 1.0. The normalized adhesion force is constant until approximately 50° then increases abruptly from 50° to 60°. The average normalized adhesion force is 3.2 when the inclination angle is over 60°. It is expected that the contact area of the CNF tip is constant until approximately 50° because the Pd sphere on the CNF is in contact with the surface of the sample as shown in Figure 9.

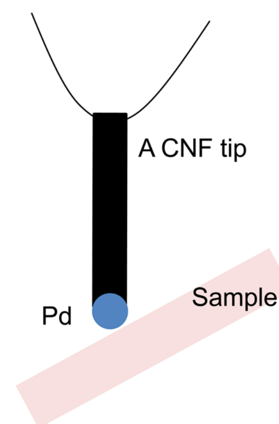

Figure 9. Schematic image of a CNF tip with a Pd nanoparticle and a sample.

Above 60°, another part of the tip may be in contact with the sample, yielding a high adhesion force. In fact, we found that it was unnecessary to correct the adhesion force by considering the angle between the tip of the cantilever and the sample for an angle of under 50°.

The SEM image in Figure 10a shows the surface of continuous nanoscale protrusions measured by a contact

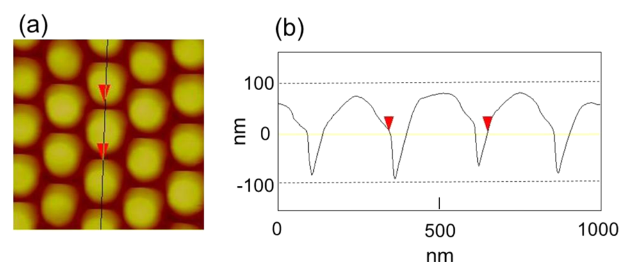

Figure 10. AFM image of continuous nanoscale protrusions. (a) Image of surface recorded by a contact−mode AFM. (b) Cross-sectional view of bell-shaped protrusions along black line in panel a.

mode AFM. The measurement sample consisted of a hydrophilic layer and a hydrophobic layer, and it was considered to have the ideal structure shown in Figure 2. Figure 10b shows the profile along the black solid line in Figure 10a, which illustrates that the CNF tip of the cantilever could follow the shape of the continuous nanoscale protrusions.

The image in Figure 11a indicates the positions at which the adhesion force was measured, which were a valley between neighboring protrusions (position A), near the base of a protrusion (position B), the slope of a protrusion (position C), and the top of a protrusion (position D). Figure 11b shows distributions of the adhesion forces for some different positions on a same film normalized by the adhesion force of hydrophobic flat planar substrate using the probe of the AFM with an attached CNF when the contact acute angle in Figure 8a between the CNF tip and the direction perpendicular to the

DOI: 10.1021/acsami.5b01307
ACS Appl. Mater. Interfaces 2015, 7, 13776−13781

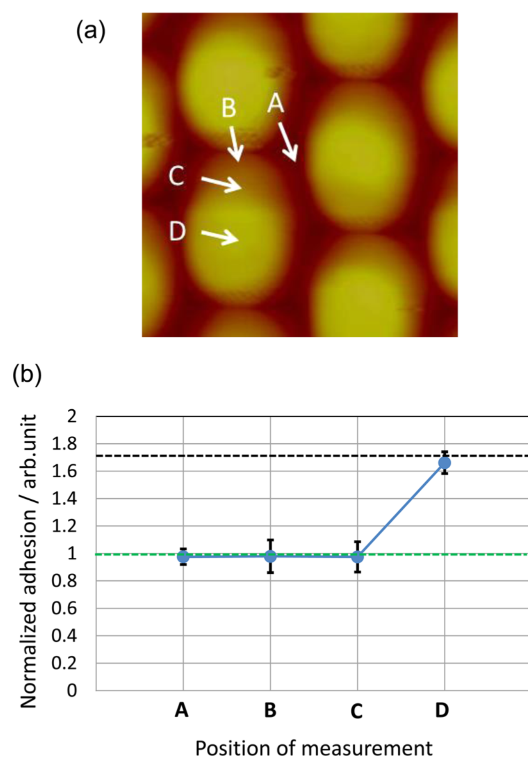

Figure 11. Normalized adhesion force distribution on nanoscale protrusions. (a) Image of surface obtained by an AFM using a CNF tip. (b) Adhesion force at different positions obtained by an AFM using the probe with an attached CNF. Position A: Valley between protrusions. Position B: Near base of a protrusion. Position C: Slope of a protrusion. Position D: Top of a protrusion.

sample is 0°. The black and green broken lines in Figure 11b are the normalized values of the adhesion forces of hydrophilic and hydrophobic flat planar substrates by the above-mentioned value of hydrophobic substrate using the probe with an attached CNF at the contact angle of 0°, respectively. We found that the adhesion force including the deviations measured using the tip with an attached CNF were obtained with low scattering. From these results, we found that the adhesion force distribution obtained by the probe with attached CNFs depends on the position in the array and that it was possible to measure the distribution of the adhesion force on the continuous nanoscale protrusions at all positions. The force at the top of an array is stronger than elsewhere; this result suggests that the hydrophilic material exists locally near the top of a protrusion, whereas the remainder of the protrusion consists of the hydrophobic material.

4. CONCLUSION

We have measured the adhesion force between a surface and a CNF tip capped with a Pd nanoparticle by recording force curves using an AFM. Because it is impossible to directly measure the nanonewton adhesion force of the surface of a film having an array of continuous nanoscale aligned protrusions, we attempted to measure the adhesion force of the bell-shaped protrusions using a CNF tip with a Pd nanoscale particle, which was synthesized on a Pd catalyst layer covering the end of a tip by PECVD. A flow for the measurement of continuous nanoscale protrusions was established to analyze the position, the displacement magnitude, and the variation of the phase, and we succeeded in measuring the adhesion force from the top to the bottom of an array of protrusions. Thus, it is possible to analyze the distribution of the adhesion force for a nanoscale protrusion between a CNF tip and sample by an AFM. The adhesion force of inclined surfaces as well as smooth surfaces can be observed, and we found that a hydrophilic layer locally existed at the top of each protrusion in our measured sample. This method for measuring the adhesion force is valuable for analyzing in detail the distribution of the adhesion force on a rough continuous structure at the nanoscale level.

■ AUTHOR INFORMATION

Corresponding Author

*Fax: +81-22-795-4584. E-mail: shimoi@mail.kankyo.tohoku.ac.jp.

Notes

The authors declare no competing financial interest.

■ ACKNOWLEDGMENTS

This work was partially supported by the Global COE Program "Materials Integration International Center of Education and Research, Tohoku University," of MEXT, Japan. The authors are indebted to members of the Technical Division, School of Engineering of Tohoku University, for discussions on the SPM experimental data. The motheye structures were prepared by DOWA Co., Ltd., who kindly donated some samples for measurements.

■ REFERENCES

(1) del Rio, F. W.; de Boer, M. P.; Knapp, J. A.; Reedy, E. D., Jr.; Clews, P. J.; Dunn, M. L. The Role of Van der Waals Forces in Adhesion of Micromachined Surfaces. *Nat. Mater.* **2005**, *4*, 629−634.
(2) Ferreira, O. D. S.; Gelinck, E.; de Graaf, D.; Fischer, H. Adhesion Experiments Using an AFM—Parameters of Influence. *Appl. Surf. Sci.* **2010**, *257*, 48−55.
(3) Endoh, S.; Hayashibe, K. Nanomold Fabrication and Nanoimprint Devices Using Advanced Blu-ray Disc Technology. *Jpn. J. Appl. Phys.* **2009**, *48*, No. 06FD04.
(4) Gombert, A.; Glaubitt, W.; Rose, K.; Dreibholz, J.; Bläsi, B.; Heinzel, A.; Sporn, D.; Döll, W.; Wittwer, V. Subwavelength-Structured Antireflective Surfaces on Glass. *Thin Solid Films* **1999**, *351*, 73−78.
(5) Kanamori, Y.; Kobayashi, K.; Yugami, H.; Hane, K. Subwavelength Antireflection Gratings for GaSb in Visible and Near-Infrared Wavelengths. *Jpn. J. Appl. Phys.* **2003**, *42*, 4020−4023.
(6) Nakanishi, T.; Hiraoka, T.; Fujimoto, A.; Saito, S.; Asakawa, K. Nano-Patterning Using an Embedded Particle Monolayer as an Etch Mask. *Microelectron. Eng.* **2006**, *83*, 1503−1508.
(7) Kurihara, K.; Saitou, Y.; Nakano, T.; Kato, H.; Tominaga, J. Nano-Structured Mold to Attain Anti-Reflection on Optical Element Surface. *14th Int. Display Workshops Dig.* **2007**, 1001.
(8) Bernhard, C. G.; Miller, W. H. A Corneal Nipple Pattern in Insect Compound Eyes. *Acta Physiol. Scand.* **1962**, *56*, 385.
(9) Chunder, A.; Etcheverry, K.; Zhai, L. Fabrication of Antireflection Coatings for Displays. *SID Int. Symp. Dig. Technol. Pap.* **2008**, *39*, 557.
(10) Schulz, U.; Munzert, P.; Leitel, R.; Wendling, I.; Kaiser, N.; Tünnermann, A. Antireflection of Transparent Polymers by Advanced Plasma Etching Procedures. *Opt. Express* **2007**, *15*, 13108−13113.
(11) Macdonald, T.; Gibson, C. T.; Constantopoulos, K.; Shapter, J. G.; Ellis, A. V. Functionalization of Vertically Aligned Carbon Nanotubes with Polystyrene via Surface Initiated Reversible Addition Fragmentation Chain Transfer Polymerization. *Appl. Surf. Sci.* **2012**, *258*, 2836−2843.
(12) Persson, B. N. J.; Tosatti, E. The Effect of Surface Roughness on the Adhesion of Elastic Solids. *J. Chem. Phys.* **2001**, *115*, 5597−5610.

(13) Watson, G. S.; Watson, J. A. Natural Nano-Structures on Insects-Possible Functions of Ordered Arrays Characterized by Atomic Force Microscopy. *Appl. Surf. Sci.* **2004**, *235*, 139−144.
(14) Chen, S. H.; Soh, A. K. The Capillary Force in Micro- and Nano-Indentation with Different Indenter Shapes. *Int. J. Solids Struct.* **2008**, *45*, 3122−3137.
(15) Paajanen, M.; Katainen, J.; Pakarinen, O. H.; Foster, A. S.; Lahtinen, J. Experimental Humidity Dependency of Small Particle Adhesion on Silica and Titania. *J. Colloid Interface Sci.* **2006**, *304*, 518−523.
(16) Fukunishi, A.; Mori, Y. Adhesion Force between Particles and Substrate in a Humid Atmosphere Studied by Atomic Force Microscopy. *Adv. Powder Technol.* **2006**, *17*, 567−580.
(17) He, M.; Blum, A. S.; Aston, D. E.; Buenviaje, C.; Overney, R. M.; Luginbühl, R. Critical Phenomena of Water Bridges in Nanoasperity Contacts. *J. Chem. Phys.* **2001**, *114*, 1355−1360.
(18) Li, Z. X.; Zhang, L. J.; Yi, H. H.; Fang, H. P. Theoretical Study on the Capillary Force between an Atomic Force Microscope Tip and a Nanoparticle. *Chin. Phys. Lett.* **2007**, *24*, 2289−2292.
(19) Asay, D. B.; Kim, S. H. Effects of Adsorbed Water Layer Structure on Adhesion Force of Silicon Oxide Nanoasperity Contact in Humid Ambient. *J. Chem. Phys.* **2006**, *124*, No. 174712.
(20) Farshchi-Tabrizi, M.; Kappl, M.; Cheng, Y.; Gutmann, J.; Butt, H. J. On the Adhesion between Fine Particles and Nanocontacts: an Atomic Force Study. *Langmuir* **2006**, *22*, 2171−2184.
(21) Pakarinen, O. H.; Foster, A. S.; Paajanen, M.; Kalinainen, T.; Katainen, J.; Makkonen, I.; Lahtinen, J.; Nieminen, R. M. Towards an Accurate Description of the Capillary Force in Nanoparticle Surface Interactions. *Model. Simul. Mater. Sci. Eng.* **2005**, *13*, 1175−1186.
(22) Butt, H. J.; Kappl, M. Normal Capillary Forces. *Adv. Colloid Interface Sci.* **2009**, *146*, 48−60.
(23) Chau, A.; Régnier, S.; Delchambre, A.; Lambert, P. Theoretical and Experimental Study of the Influence of AFM Tip Geometry and Orientation on Capillary Force. *J. Adhes. Sci. Technol.* **2010**, *24*, 2499−2510.
(24) Feiler, A. A.; Stiernstedt, J.; Theander, K.; Jenkins, P.; Rutland, M. W. Effect of Capillary Condensation on Friction Force and Adhesion. *Langmuir* **2007**, *23*, 517−522.
(25) Weeks, B. L.; Vaughn, M. W.; DeYoreo, Y. Y. Direct Imaging of Meniscus Formation in Atomic Force Microscopy using Environmental Scanning Electron Microscopy. *Langmuir* **2005**, *21*, 8096−8098.
(26) Sabadi, M.; Kettle, J.; Rautkoski, H.; Claesson, P. M.; Thormann, E. Structural and Nanomechanical Properties of Paperboard Coatings Studied by Peak Force Tapping Atomic Force Microscopy. *ACS Appl. Mater. Interfaces* **2012**, *4*, 5534−5541.
(27) Duner, G.; Thormann, E.; Dedinaite, A.; Claesson, P. M.; Matyjaszewski, K.; Tilton, R. D. Nanomechanical Mapping of a High Curvature Polymer Brush Grafted from a Rigid Nanoparticle. *Soft Matter.* **2012**, *8*, 8312−8320.
(28) Ando, Y. The Effect of Relative Humidity on Friction and Pull-off Forces Measured on Submicron-Size Asperity Arrays. *Wear* **2000**, *238*, 12−19.
(29) Colak, A.; Wormeester, H.; Zandvliet, H. J. W.; Poelsema, B. Surface Adhesion and Its Dependence on Surface Roughness and Humidity Measured with a Flat AFM Tip. *Appl. Surf. Sci.* **2012**, *258*, 6938−6942.
(30) Gibson, C. T.; Carnally, S.; Roberts, C. J. Attachment of Carbon Nanotubes to Atomic Force Microscope Probes. *Ultramicroscopy* **2007**, *107*, 1118−1122.
(31) Slattery, A. D.; Blanch, A. J.; Quinton, J. S.; Gibson, G. T. Efficient Attachment of Carbon Nanotubes to Conventional and High-Frequency AFM Probes Enhanced by Electron Beam Processes. *Nanotechnology* **2013**, *24*, No. 235705.
(32) Tanemura, M.; Iwata, K.; Takahashi, K.; Fujimoto, Y.; Okuyama, F.; Sugie, H.; Filip, V. Growth of Aligned Carbon Nanotubes by Plasma-Enhanced Chemical Vapor Deposition: Optimization of Growth Parameters. *J. Appl. Phys.* **2001**, *90*, 1529−1533.
(33) Kita, S.; Sakai, Y.; Fukushima, T.; Mizuta, Y.; Ogawa, A.; Senda, S.; Okuyama, F. Characterization of Field-Electron Emission from Carbon Nanofibers Grown on Pd Wire. *Appl. Phys. Lett.* **2004**, *85*, 4478−4480.
(34) Cleveland, J. P.; Manne, S.; Bocek, D.; Hansma, P. K. A Nondestructive Method for Determining the Spring Constant of Cantilevers for Scanning Force Microscopy. *Rev. Sci. Instrum.* **1993**, *64*, 403−405.
(35) Sader, J. E.; Larson, I.; Mulvaney, P.; White, L. R. Method for the Calibration of Atomic Force Microscope Cantilevers. *Rev. Sci. Instrum.* **1995**, *66*, 3789−3798.
(36) Slattery, A. D.; Blanch, A. J.; Quinton, J. S.; Gibson, C. T. Accurate Measurement of Atomic Force Microscope Cantilever Deflection Excluding Tip-Surface Contact with Application to Force Calibration. *Ultramicroscopy* **2013**, *131*, 46−55.
(37) Slattery, A. D.; Quinton, J. S.; Gibson, C. T. Atomic Force Microscope Cantilever Calibration Using a Focused Ion Beam. *Nanotechnology* **2012**, *23*, No. 285704.
(38) Slattery, A. D.; Blanch, A. J.; Quinton, J. S.; Gibson, C. T. Calibration of Atomic Force Microscope Cantilevers Using Standard and Inverted Static Methods Assisted by FIB-Milled Spatial Markers. *Nanotechnology* **2013**, *24*, 015710.
(39) Slattery, A. D.; Blanch, A. J.; Ejov, V.; Quinton, J. S.; Gibson, C. T. Spring Constant Calibration Techniques for Next-Generation Fast-Scanning Atomic Force Microscope Cantilevers. *Nanotechnology* **2014**, *25*, No. 335705.

DOI: 10.1021/acsami.5b01307
ACS Appl. Mater. Interfaces 2015, 7, 13776−13781